6th International Conference on Advances in Experimental Structural Engineering
11th International Workshop on Advanced Smart Materials and Smart Structures Technology
August 1-2, 2015, University of Illinois, Urbana-Champaign, United States

Road Roughness Evaluation With In-Pavement Sensors

Z. Zhang[1], F. Deng[2], Y. Huang[3], and R. Bridgelall[4]

1 *Research Assistant, Dept. of Civil and Environmental Engineering, North Dakota State University, Fargo, United States. E-mail: zhiming.zhang@ndsu.edu*
2 *Teaching Assistant, Dept. of Civil and Environmental Engineering, North Dakota State University, Fargo, United States. E-mail: fodan.deng@ndsu.edu*
3 *Assistant Professor, Dept. of Civil and Environmental Engineering, North Dakota State University, Fargo, United States. E-mail: ying.huang@ndsu.edu*
4 *Program Director, Upper Great Plains Transportation Institute, North Dakota State University, Fargo, United States. E-mail: raj.bridgelall@ndsu.edu*

ABSTRACT
Most transportation agencies now collect pavement roughness data using the inertial profilers. Road profiling activities require instrumented vehicles and technicians with specialized training to interpret the results, which is expensive and, therefore, limits data collection to at most once per year for portions of the national highway system. Agencies characterize roughness only for some secondary roads but much less frequently. This paper developed a method linking the output of durable in-pavement strain sensors to road roughness level by theoretical derivation and numerical simulation. The durable in-pavement sensors will continuously provide information of road roughness after they are installed and calibrated during the road construction. Without the high cost for profiling facilities and technicians, this approach will serve as an economic solution after recovering the initial cost.

KEYWORDS: *road roughness, strain sensors, dynamic wheel load*

1. INTRODUCTION

Roughness, a global measure of roadway serviceability, has been long used as one of the major criteria for road condition assessment and maintenance resource allocation. The ASTM E867 standard defines roughness as the deviation of a surface from a true planar surface with characteristic dimensions that affect vehicle dynamics and ride quality [1]. Pavement roughness adversely affects vehicle wear, ride quality, and transportation safety [2]. The higher dynamic axle loading from roughness accelerates pavement deterioration [3]. Rough roads can also increase fuel consumption by as much as 4-5 percent [4].

According to NCHRP Report 334 [5], most transportation agencies now collect pavement roughness data using the automated systems mentioned above, especially the inertial profilers, for at least part of their paved roadway network. The literature has very little information about the cost of using such inertial profilers. One study reported pavement profile data collection and analysis costs in the range of $2.23 - $10.00/mile with an average cost of $6.12/mile [6]. In general, the relatively high expense and labor requirements of existing approaches prevent agencies from monitoring large portions of their roadway network more often than once annually. Thus, they often make maintenance and rehabilitation decisions based on outdated roughness data. In addition, infrequent roughness measurements preclude the identification of dangerous distress symptoms such as frost heaves that appear and disappear between annual monitoring cycles. These situations result in roadway safety gaps that increase liability.

This paper introduces a new approach to evaluate and report pavement roughness by linking the output of in-pavement strain sensors to the road roughness level. This approach contains two different algorithms that provide the international roughness index (IRI) and the power spectra density (PSD) of the road profile, respectively. This method requires initial installation of the durable strain sensors inside the pavement during the road construction stage. During road operation, the sensors report strain data that indicates the level of roughness development. The method developed in this study will subsequently produce the roughness information. After agencies recover the initial cost of sensor deployment and calibration by removing the need for future expensive profiling activities, they will begin to benefit from the reduced cost of roughness monitoring activities throughout the remaining life cycle of the pavement assets.

The organization of the remaining paper is as follows: Section 2 develops the theoretical method that quantifies the road roughness by using the output of the in-pavement strain sensors. Section 3 is numerical simulation. Finally, Section 4 provides the conclusion and outlines the potential future work.

2. THEORETICAL ANALYSIS

2.1. Relationship between IRI and Pavement Strains

A deformation-induced increase of strain within the pavement structure corresponds to an accumulation of profile unevenness, because a deformation of the pavement structure would produce a change in the road profile.

2.1.1 Relationship between in-pavement strains and roughness for concrete-paved roads

According to the Kirchhoff–Love plate theory [7], the strain in the longitudinal (x) direction of a thin-plate concrete panel, ε_x, located inside the pavement at some known vertical position h_0, is expressed as:

$$\varepsilon_x = -h_0 \frac{d^2 w}{dx^2}, \tag{2.1}$$

where w is the vertical displacement of the concrete pavement panel which is also known as the road elevation profile. With the sampling interval requirement satisfied, double integration of Eq. 2.1 reproduces the relation between the road elevation profile and the measured strains from the in-pavement sensors as:

$$w = -\iint \frac{\varepsilon_x}{h_0} dx. \tag{2.2}$$

The IRI then becomes available because the slope rate of the road profile, $\ddot{w}$, which is the second derivative of the elevation profile w with respect to time, is a direct input to the procedure that computes the IRI. For a temporal road profile of ξ, the second derivative with respect to time is

$$\ddot{\xi} = -\ddot{w} = \frac{v^2 \varepsilon_x}{h_0} \tag{2.3}$$

where v = 80 km/h is the IRI standard speed [8].

2.1.2 IRI calculation based on in-pavement strains

The Highway Safety Research Institute (HSRI) defines the IRI in terms of the responses from a standard quarter-vehicle model having two degrees of freedom as shown in Fig. 2.1.

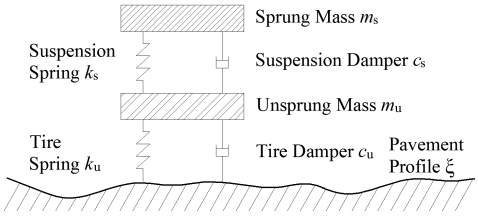

Figure 2.1 The HSRI quarter-vehicle model

The HSRI quarter-car parameters are k_u/m_s = 653.0 s^{-2}, k_s/m_s = 63.3 s^{-2}, m_u/m_s = 0.15, c_s/m_s = 6.0 s^{-1} and c_u/m_s = 0.0 s^{-1}. Assume that parameters y^t_s and y^t_u are absolute displacements of the sprung and unsprung mass, respectively, then the relative displacement of sprung mass y_s and that of the unsprung mass y_u are

$$y_s = y^t_s - y^t_u \qquad \text{and} \qquad y_u = y^t_u - \xi. \tag{2.4}$$

Expressed in matrix-form, the ordinary differential equations to define the system dynamics for the sprung and unsprung mass is

$$M\ddot{Y}(t)+C\dot{Y}(t)+KY(t)=R(t) \tag{2.5}$$

where

$$M=\begin{bmatrix} m_s & m_s \\ 0 & m_u \end{bmatrix}, C=\begin{bmatrix} c_s & 0 \\ -c_s & c_u \end{bmatrix}, K=\begin{bmatrix} k_s & 0 \\ -k_s & k_u \end{bmatrix},$$
$$\ddot{Y}=\begin{Bmatrix} \ddot{y}_s \\ \ddot{y}_u \end{Bmatrix}, \dot{Y}=\begin{Bmatrix} \dot{y}_s \\ \dot{y}_u \end{Bmatrix}, Y=\begin{Bmatrix} y_s \\ y_u \end{Bmatrix}, \text{and } R=\begin{Bmatrix} -m_s\ddot{\xi} \\ -m_u\ddot{\xi} \end{Bmatrix} \tag{2.6}$$

Substituting Eq. 2.3 into Eq. 2.6 provides the expression:

$$R=\begin{Bmatrix} -m_s\dfrac{v^2\varepsilon_x}{h_0} \\ -m_u\dfrac{v^2\varepsilon_x}{h_0} \end{Bmatrix} \tag{2.7}$$

Solving Eq. 2.5 with a numerical algorithm such as the Newmark method yields the relative displacements y_s and y_u, the relative velocities $\dot{y}_s$ and $\dot{y}_u$, and the relative accelerations $\ddot{y}_s$ and $\ddot{y}_u$ as a function of the in-pavement strains and velocities of the vehicle. The IRI is then [8]:

$$\text{IRI}=\frac{1}{L}\int_0^T|\dot{y}_s|\mathrm{d}t \tag{2.8}$$

in which, L is the segment length and $T = L/v$ is the travel time. For a computational sample interval of Δt, the number of intervals is $n = T/\Delta t$ and the discrete-time form of the computation becomes

$$\text{IRI}=\frac{1}{vn\Delta t}\sum_{i=0}^{n}|\dot{y}_s(t_i)|\Delta t=\frac{1}{vn}\sum_{i=0}^{n}|\dot{y}_s(t_i)| \tag{2.9}$$

2.2. Relationship between PSD of Road Roughness and Pavement Strains

2.2.1. PSD of road roughness

Numerous measurements indicates that roughness can be modelled as a uniform random field in the spatial domain [9]. Instead of varying with time, the height of road surface, ξ, varies with special distance along the road. Low frequency components correspond to long wavelength road profile, and high frequency components to short wavelength road profile. When a vehicle travels along the road at a constant speed v, a uniform random field in spatial domain is converted into a normal stationary ergodic random process in time domain. PSDs of road roughness have the relationship as

$$G_\xi(\Omega)=vG_\xi(f)=4\pi S_\xi(\omega), \tag{2.10}$$

where $\omega = 2\pi f = 2\pi v\Omega$, $G_\xi(\Omega)$ is the single-sided wave number spectrum, the so-called wave number Ω represents spatial frequency and is given by $\Omega = 1/\lambda$, where λ is the wavelength of road surface roughness, $G_\xi(f)$ and $S_\xi(\omega)$ are respective single-sided and double-sided PSD functions of road surface roughness defined by natural frequency (i.e. temporal frequency) f and angular frequency (i.e. circular frequency) ω, respectively [10].

It has been found that most pavement profiles such as road surface roughness and runway roughness have very similar form of PSD [11]. The commonly used form for representing PSD of road surface is

$$G_\xi(\Omega)=C_{SP}\Omega^{-\gamma}, \tag{2.11}$$

where C_{SP} is the roughness index, exponent γ is the parameter which controls the frequency component of PSD in frequency domain [11].

2.2.2. Dynamic wheel load of a quarter vehicle

Preceding researches indicate that a quarter vehicle model is a good representation for analysis on road roughness, ride quality, and vehicle load [12]. Taking the Fourier transform of Eq. 2.5, the frequency response equation of the quarter vehicle is

$$\begin{bmatrix} \omega^2 - \dfrac{\mathrm{i}\omega c_\mathrm{u}}{m_\mathrm{u}} - \dfrac{k_\mathrm{u}}{m_\mathrm{u}} & \dfrac{\mathrm{i}\omega c_\mathrm{s}}{m_\mathrm{u}} + \dfrac{k_\mathrm{s}}{m_\mathrm{u}} \\ \omega^2 & \omega^2 - \dfrac{\mathrm{i}\omega c_\mathrm{s}}{m_\mathrm{s}} - \dfrac{k_\mathrm{s}}{m_\mathrm{s}} \end{bmatrix} \begin{bmatrix} H_\mathrm{u}(\omega) \\ H_\mathrm{s}(\omega) \end{bmatrix} = \begin{bmatrix} \omega^2 \\ \omega^2 \end{bmatrix}, \tag{2.12}$$

where $H_\mathrm{s}(\omega) = \mathcal{F}(y_\mathrm{s})/\mathcal{F}(\xi)$ and $H_\mathrm{u}(\omega) = \mathcal{F}(y_\mathrm{u})/\mathcal{F}(\xi)$ are the frequency response of the sprung and unsprung mass, respectively, and the function $\mathcal{F}(x)$ indicates the Fourier transform operation of x. From the quarter vehicle model, the dynamic wheel load can be expressed as

$$P(t) = k_\mathrm{u} y_\mathrm{u}(t) + c_\mathrm{u} \dot{y}_\mathrm{u}(t) \tag{2.13}$$

Taking the Fourier transform on both sides of Eq. 2.13 and using linear system theory [13], the PSD of dynamic wheel load (DWL) $S_P(\omega)$ is

$$S_P(\omega) = A(\omega) S_\xi(\omega) \tag{2.14}$$

where $A(\omega) = |(k_\mathrm{u} + \mathrm{i}c_\mathrm{u}\omega)\mathrm{H}_\mathrm{u}(\omega)|^2$.

2.2.3. Description of road roughness with pavement strains

The strain signal $I(t)$ captured by sensors deployed inside the pavement is a convolution of the linear load function $P_\mathrm{L}(t)$ and the sensor's sensitivity function $T(t)$ multiplied by the vehicle's travelling speed [14], as is shown in Eq. 2.15.

$$I(t) = \int_{-\infty}^{+\infty} P_\mathrm{L}(t-\tau) T(\tau) v \mathrm{d}\tau \tag{2.15}$$

A common practice is to take the dynamic wheel load $P(t)$ as a concentrated point load for simplicity [10], then it can be expressed as the product of the amplitude P_0 and a Dirac-delta function $\delta(t)$. Then Eq. 2.15 becomes

$$I(t) = P_0 T(t). \tag{2.16}$$

The maximum strain I_0 when a vehicle tire traverses a specific sensor is proportional to the load magnitude P_0, that is

$$I_0 = \alpha P_0, \tag{2.17}$$

and the coefficient α is maximum of the sensor's sensitivity function.

When the vehicle travel along the road path with strain sensors deployed inside the pavement underneath, the strain history $I_0(t)$ that is the series of the maximum strains collected from the sensors is proportional to the history of the dynamic wheel load $P_0(t)$, as is shown in Eq. 2.18.

$$I_0(t) = \alpha P_0(t) \tag{2.18}$$

By linear system theory, the PSD of the $I_0(t)$, $S_I(\omega)$, and the PSD of $P_0(t)$, $S_P(\omega)$, have the relationship as

$$S_P(\omega) = \frac{S_I(\omega)}{\alpha^2} \tag{2.19}$$

Substituting Eq. 2.19 into Eq. 2.14, the PSD of road roughness $S_\xi(\omega)$ can be expressed with the transfer function

$A(\omega)$ and the PSD of the strain history $S_I(\omega)$, as is shown in Eq. 2.20.

$$S_{\xi}(\omega) = \frac{S_I(\omega)}{\alpha^2 A(\omega)} \tag{2.20}$$

In addition, Sun developed the relation between the DWL's coefficient of variation λ_P and the roughness index C_{SP} as

$$\lambda_P = \frac{\beta}{\overline{P}}\sqrt{vC_{SP}} \tag{2.21}$$

where $\beta = \int_0^{\infty} [A(\omega = 2\pi f)]^{0.5} / f df$, and $\overline{P}$ is the static wheel load [15]. As the strain history $I_0(t)$ is proportional to the load history $P(t)$, the roughness index can be expressed with $I_0(t)$'s coefficient of variation λ_I and the strain value from the static wheel load $\overline{I}$, as is shown in Eq. 2.22.

$$C_{SP} = \frac{1}{v}\left(\frac{\lambda_I \overline{I}}{\alpha\beta}\right)^2 \tag{2.22}$$

Though this method can't acquire the road profile that is the fundamental data for roughness evaluation, the PSD of road profile is also an important evaluation, and preceding researches explored the method to link the PSD to the widely used roughness statistic IRI [16]. Thus the strain method is prospective to give a comprehensive evaluation of road roughness condition.

3. NUMERICAL SIMULATION

This section conducts numerical simulation to the method described in Section 2. **3.1** corresponds to the algorithm in **2.1**, and **3.2** to **2.2**, respectively.

3.1. IRI and Pavement Strains

Fig. 3.1 a is the generated roughness at C_{SP} = 6.4×10^{-5} m^3/cycle for a road section of 1000 m by the IFFT method [17, 18]. Assume that the location of the deployed strain sensors are at h_0 = 0.02 m. Fig. 3.1 b is the corresponding strain series calculated by Eq. 2.1. By the quarter-vehicle algorithm displayed in **2.1**, the value of IRI for this road section is 6.98.

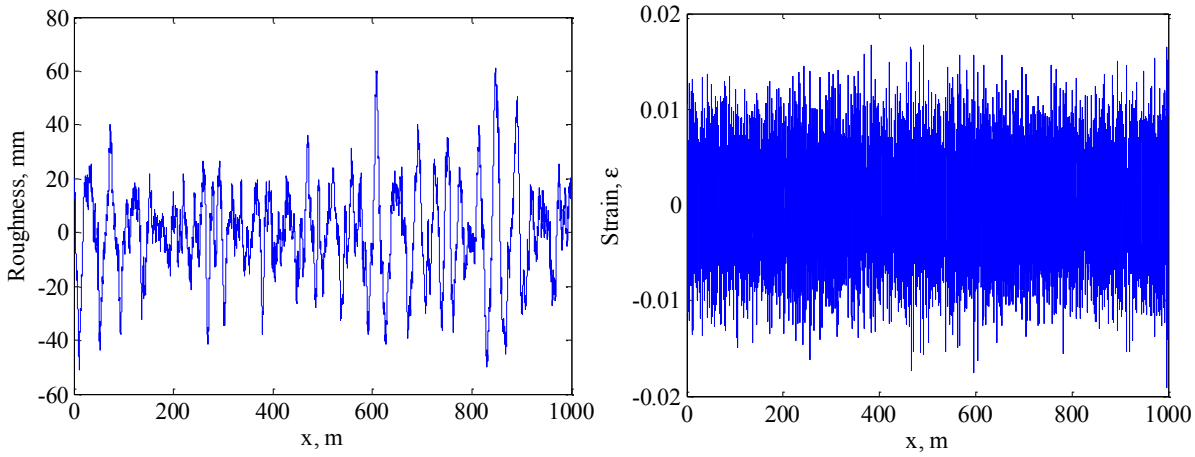

(a) Roughness (b) Strain series

Figure 3.1 Generated roughness at C_{SP} = 64 and the corresponding strains at h_0 = 0.02 m

3.2. PSD and Pavement Strains

This numerical simulation uses the same road roughness level and profile with those in **3.1** that is repeated in Fig. 3.2 a. Tab. 3.1 lists all the parameters for the dynamic wheel load (DWL) calculation. Fig. 3.2 b is the DWL calculated with Eq. 2.13.

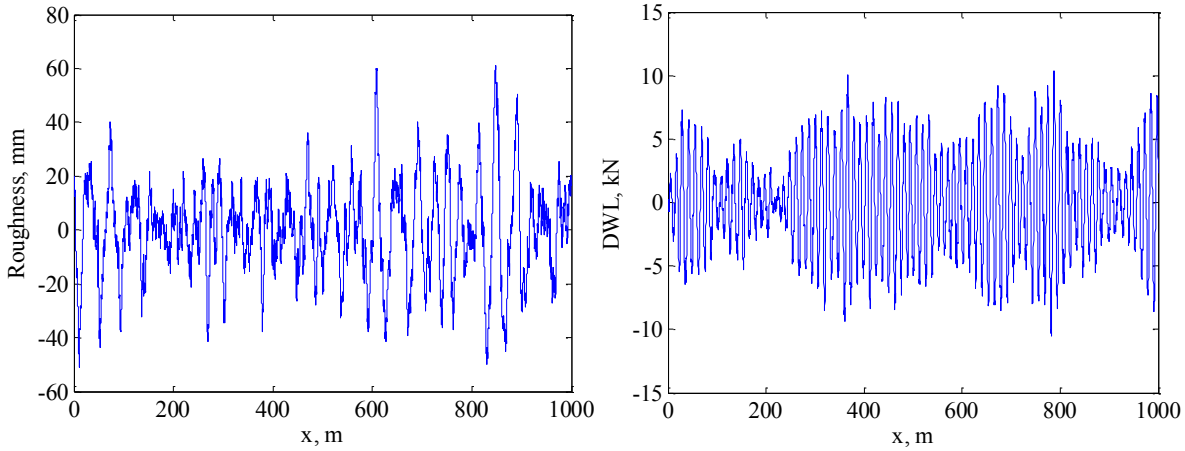

(a) Roughness (b) DWL

Figure 3.2 Generated roughness at C_{SP} = 64 and the corresponding dynamic load

Table 3.1 Parameters used for numerical simulation

Parameters	Description of parameters	Values
m_s	mass of sprung mass, kg	578
m_u	mass of unpsrung mass, kg	32
k_s	stiffness of the suspension spring, N/m	118490
k_u	stiffness of the tire spring, N/m	165372
c_s	damping coefficient of the sprung mass, Ns/m	300
c_u	damping coefficient of the unsprung mass, Ns/m	302
v	speed, m/s,	22.22

Assuming that the coefficient in Eq. 2.17 is $\alpha = 10^{-2}$ με/N, Fig. 3.3 a is the strain series. Fig. 3.3 b is the PSD of the strains calculated with the Welch's overlapped segment averaging estimator. This spectra reflects the frequency characteristics of the road roughness interacting with the given quarter vehicle system. With the transfer function in Eq. 2.14 $A(\omega)$ know, the PSD of road roughness can be calculated by Eq. 2.20.

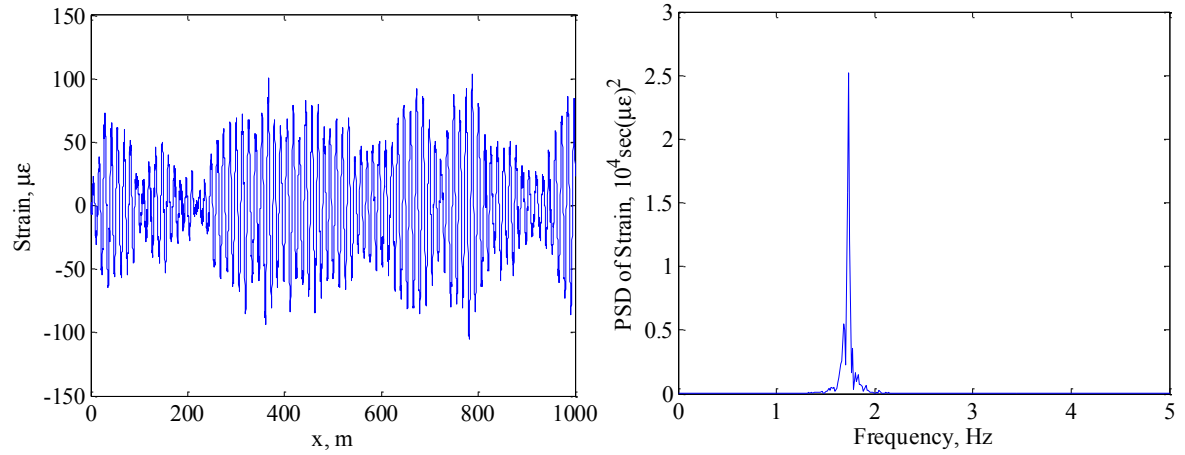

(a) Strain series (b) PSD of Strain

Figure 3.2 Strain series at $\alpha = 10^{-2}$ με/N and its PSD

4. CONCLUSIONS AND FUTURE WORK

This paper provides transportation researchers and engineers with a cost-effective method of road roughness evaluation using strain sensors deployed inside the pavement. The authors conducted theoretical derivation to develop the relation between the measured strains from the in-pavement strain sensors and the road roughness condition, followed by numerical simulation. The conclusions of this paper are as follows:

1) With different algorithms, both the IRI and PSD of a specific road section can be derived from strain series inside the pavement.

2) Numerical simulation gives a brief view of this new method and provides a guidance for future field experiments.

Future work will spend more efforts on field validation, and it is prospective to extend this method to the application on bridges.

ACKNOWLEDGEMENT
A USDOT UTC grant under MPC agreement DTRT12-G-UTC08 provided funding for this study. The findings and opinions expressed in this article are those of the authors only and do not necessarily reflect the views of the sponsors. The authors sincerely thank Mr. Robert Strommen and Mr. Leonard Palek from MnROAD, MnDOT for their assistance.

REFERENCES

1. ASTM. (2012), E867 Standard terminology relating to vehicle-pavement systems, American Society for Testing Materials.
2. Brickman, A.D., et al. (1972), Road roughness effects on vehicle performance, Transportation Research Board.
3. Saleh, M.F., M.S. Mamlouk, and E.B. Owusu-Antwi. (2000). Mechanistic roughness model based on vehicle-pavement interaction. *Transportation Research Record: Journal of the Transportation Research Board*. **1699: 1**, 114-120.
4. Klaubert, E.C. (2001). Highway effects on vehicle performance, Transportation Research Board.
5. Hyman, W.A., et al. (1990). Improvements in data acquisition technology for maintenance management systems, Transportation Research Board.
6. McGhee, K.H. (2004), Automated pavement distress collection techniques, Transportation Research Board.
7. Timoshenko, S., S. Woinowsky-Krieger, and S. Woinowsky-Krieger. (1959), Theory of plates and shells, McGraw-hill New York.
8. ASTM. (2008), E1926 Standard practice for computing international roughness index of roads from longitudinal profile measurements, American Society for Testing Materials.
9. Newland, D.E. (2012), An introduction to random vibrations, spectral & wavelet analysis, Courier Corporation.
10. Sun, L. and X. Deng. (1998). Predicting vertical dynamic loads caused by vehicle-pavement interaction. *Journal of transportation engineering*. **124: 5**, 470-478.
11. Cebon, D. (1999), Handbook of vehicle-road interaction, Transportation Research Board.
12. Todd, K.B. and B.T. Kulakowski. (1989), Simple computer models for predicting ride quality and pavement loading for heavy trucks, Transportation Research Record.
13. Lathi, B.P. (2009), Linear systems and signals, Oxford University Press.
14. Zhang, Z., et al. (2015). Sampling optimization for high-speed weigh-in-motion measurements using in-pavement strain-based sensors. *Measurement Science and Technology*. **26: 6**, 065003.
15. Sun, L. (2001). Computer simulation and field measurement of dynamic pavement loading. *Mathematics and computers in simulation*. **56: 3**, 297-313.
16. Sun, L., Z. Zhang, and J. Ruth. (2001). Modeling indirect statistics of surface roughness. *Journal of transportation engineering*. 1**27: 2**, 105-111.
17. Wu, J.J. (2000). Simulation of rough surfaces with FFT. *Tribology International*, **33: 1**, 47-58.
18. Jiang, C.D., et al. (2012). Simulation of road roughness based on using IFFT method. *in Software Engineering (WCSE), 2012 Third World Congress on*. *IEEE*, China.